

University of Groningen

Peroxisomal membrane contact sites in the yeast *Hansenula polymorpha*

Aksit, Arman

IMPORTANT NOTE: You are advised to consult the publisher's version (publisher's PDF) if you wish to cite from it. Please check the document version below.

Document Version

Publisher's PDF, also known as Version of record

Publication date:
2018

[Link to publication in University of Groningen/UMCG research database](#)

Citation for published version (APA):

Aksit, A. (2018). *Peroxisomal membrane contact sites in the yeast Hansenula polymorpha*. [Thesis fully internal (DIV), University of Groningen]. University of Groningen.

Copyright

Other than for strictly personal use, it is not permitted to download or to forward/distribute the text or part of it without the consent of the author(s) and/or copyright holder(s), unless the work is under an open content license (like Creative Commons).

The publication may also be distributed here under the terms of Article 25fa of the Dutch Copyright Act, indicated by the "Taverne" license. More information can be found on the University of Groningen website: <https://www.rug.nl/library/open-access/self-archiving-pure/taverne-amendment>.

Take-down policy

If you believe that this document breaches copyright please contact us providing details, and we will remove access to the work immediately and investigate your claim.

Downloaded from the University of Groningen/UMCG research database (Pure): <http://www.rug.nl/research/portal>. For technical reasons the number of authors shown on this cover page is limited to 10 maximum.

Chapter 4

Pex25 is essential for peroxisome growth in *pex11* cells

Arman Akşit, Anita M. Kram and Ida J. van der Klei

Abstract

Pex11 and Pex25 are peroxisomal membrane proteins that belong to the same protein family. Recent studies in the yeast *Hansenula polymorpha* suggest that Pex11 and Pex25 play redundant roles in peroxisome biogenesis, because cells of a *H. polymorpha pex11 pex25* double deletion strain, but not of a *pex11* single deletion strain, have a severe peroxisome biogenesis defect. Pex11 has been studied extensively, but very little is known on the function of Pex25.

Here we show that deletion of *H. polymorpha PEX25* only has a minor effect on peroxisome number, however, *pex25* cells show reduced growth on methanol, a substrate that requires functional peroxisomes. Analysis of *H. polymorpha pex11 pex25* cells revealed the presence of clusters of small peroxisomes to which peroxisomal membrane proteins are normally sorted. Also, these structures contain some matrix protein, but the bulk is mislocalized to the cytosol. Upon reintroduction, Pex25 sorts to these organelles, which subsequently mature into normal peroxisomes. At these conditions, the peroxisomes are invariably closely associated with the vacuole and nucleus.

pex25, but not *pex11* cells show abnormal vacuolar morphology. Fluorescence microscopy revealed that Pex25 is localized over the entire peroxisomal surface, but also can form patches at membrane contact sites between peroxisomes and vacuoles. Together these data suggest that Pex25 may play a role in Vacuolar-Peroxisome membrane CONTACT Sites (VAPCONS).

Introduction of an artificial peroxisome-ER linker protein results in partial suppression of the *pex11 pex25* phenotype. Based on these observations we speculate that in *pex11 pex25* both ER-Peroxisome CONTACT Sites (EPCONS) (due to the absence of Pex11) and VAPCONS (caused by *PEX25* deletion) are disturbed.

Introduction

Peroxisomes are ubiquitous organelles that perform various metabolic processes and are present in almost all eukaryotic cells. β -oxidation of fatty acids and degradation of hydrogen peroxide by catalase take place in these organelles (for a recent review see (Smith and Aitchison, 2013)). There are different models about the origin of peroxisomes ranging from *de novo* peroxisome formation from the endoplasmic reticulum (ER) to proliferation of pre-existing peroxisomes by fission (Smith and Aitchison, 2013). Peroxisome proliferation in wild-type (WT) yeast cells most likely occurs via growth and division (Motley and Hettema, 2007; Nagotu et al., 2008b).

In yeast proteins of the Pex11, Pex23 and Pex24 protein families have been proposed to be involved in peroxisome proliferation (Kiel et al., 2006). Of these proteins, the structure and function of Pex11 has been extensively studied (Erdmann and Blobel, 1995; Huber et al., 2012; Tam et al., 2003; Opaliński et al., 2011). It was shown that Pex11 contains an amphipathic α -helix which is responsible for membrane curvature that is required for peroxisome elongation prior to fission (Opaliński et al., 2011). Besides its role in peroxisomal fission Pex11 has also been affiliated with several other functions such as fatty acid oxidation and transport, peroxisome inheritance and reorganization of peroxisomal membrane proteins (PMPs) (Erdmann and Blobel, 1995; Marshall et al., 1995; Cepińska et al., 2011).

Many organisms have at least one additional Pex11-like protein. In *Saccharomyces cerevisiae* the Pex11 protein family contains three members, namely Pex11, Pex25 and Pex27 (Kiel et al., 2006). Similar to Pex11, the absence of Pex25 or Pex27 results in enlarged peroxisomes in *S. cerevisiae*. Also, overexpression of *PEX11*, *PEX25* or *PEX27* leads to increased numbers of small peroxisomes indicating that these PMPs regulate peroxisome size and number (Smith et al., 2002; Rottensteiner et al., 2003; Tam et al., 2003). Although neither one of the Pex11 family members are essential for peroxisome biogenesis in *S. cerevisiae*, Pex11 and Pex25 are both important for growth on oleate containing media (Tam et al., 2003; Huber et al., 2012). Supporting that, deletion of *PEX11* in *pex25 pex27* cells worsens the partial growth defect and blocks growth on all fatty acids (Rottensteiner et al., 2003). It was also shown that Pex25 is required for the reintroduction of peroxisomes in *S. cerevisiae pex3 pex11 pex25 pex27* cells upon induction of the *PEX3* gene (Huber et al., 2012). However, the exact function of Pex25 remains speculative.

Previously it was shown that peroxisomes in *H. polymorpha* form intimate contacts with the ER (EPCONS) and vacuoles (VAPCONS) at conditions of strong peroxisome proliferation, where VAPCONS forming the largest contacts (Chapter 3, this thesis). Also, similar to what is known for mitochondrial membrane

contact sites (MCSs), these peroxisomal MCSs most likely show redundancy. That is, simultaneous loss of EPCONS and VAPCONS component possibly causes a severe defect in growth of the peroxisomal membrane (Chapter 2 and 3, this thesis).

It was shown that *H. polymorpha* Pex11, Pex23 and Pex24 proteins are important for EPCONS which are involved in organelle expansion (Chapter 2, this thesis). Transposon mutagenesis studies of a *Hp pex11* single deletion cells revealed that deletion of *VPS13* or *PEX25* in *pex11* cells results in peroxisome deficiency (Chapter 2, this thesis). Further analysis of the phenotype of *H. polymorpha pex11 vps13* cells, revealed the presence of small peroxisomes, which upon expression of an artificial ER-peroxisome linker protein (ERPER) increased in size (Chapter 2).

We now analyzed the *Hp pex11 pex25* double mutant in more detail. We show that a *H. polymorpha pex25* single deletion strain is not affected in terms of peroxisome numbers. However, similar to *pex11 vps13* cells, *pex11 pex25* cells also contain small peroxisomes together with mislocalizations of the bulk of the matrix proteins to the cytosol. Also, the introduction of an artificial ER-peroxisome tethering protein partially suppressed the phenotype of *pex11 pex25* double mutant cells. Further studies indicated that Pex25 may play a role in regulation of VAPCONS, because Pex25 can form patches at VAPCONS and *pex25* cells have increased peroxisome-vacuole associations. Based on these observations we speculate that failure of peroxisome membrane expansion in *pex11 pex25* cells is caused by defects in both EPCONS (caused by *PEX11* deletion) and VAPCONS (caused by *PEX25* deletion).

Results

Deletion of *PEX25* in *pex11* cells results in peroxisome deficiency

In order to better understand the *pex11 pex25* phenotype we first analyzed peroxisome biogenesis and abundance in the *pex11 pex25* double deletion strains using the *pex11* and *pex25* single deletion strains as well as a WT strain as controls. Confocal Laser Scanning Microscopy (CLSM) of cells producing the peroxisomal matrix marker GFP-SKL revealed that in glucose grown cells the number of fluorescent spots, representing peroxisomes that have imported GFP-SKL, decreased in all mutant strains, with the largest reduction in the *pex11 pex25* double mutant. Cells lacking such spots showed cytosolic GFP fluorescence (**Fig. 1A, D**). Quantification of the distribution of peroxisome numbers indicated that especially the number of cells without peroxisomes dramatically increased in *pex11 pex25* cells relative to the single deletion strains (**Fig. 1A, C**).

The same deletion strains were analyzed also under peroxisome inducing condition, namely upon incubation of cells in media containing methanol (**Fig. 1B**). Relative to the WT control, peroxisome numbers were reduced in methanol-grown *pex11* and *pex11 pex25* cells, but not in *pex25* cells (**Fig. 1 B, D**). Upon deletion of both genes, cells containing peroxisomes were almost undetectable (less than 1% of the cells contain a peroxisome) (**Fig. 1B, D**).

Growth experiments indicated that all mutant strains normally grew on glucose. In methanol containing media *pex11* and *pex25* cells showed reduced growth, whereas *pex11 pex25* cells were unable to grow (**Fig. 1E**).

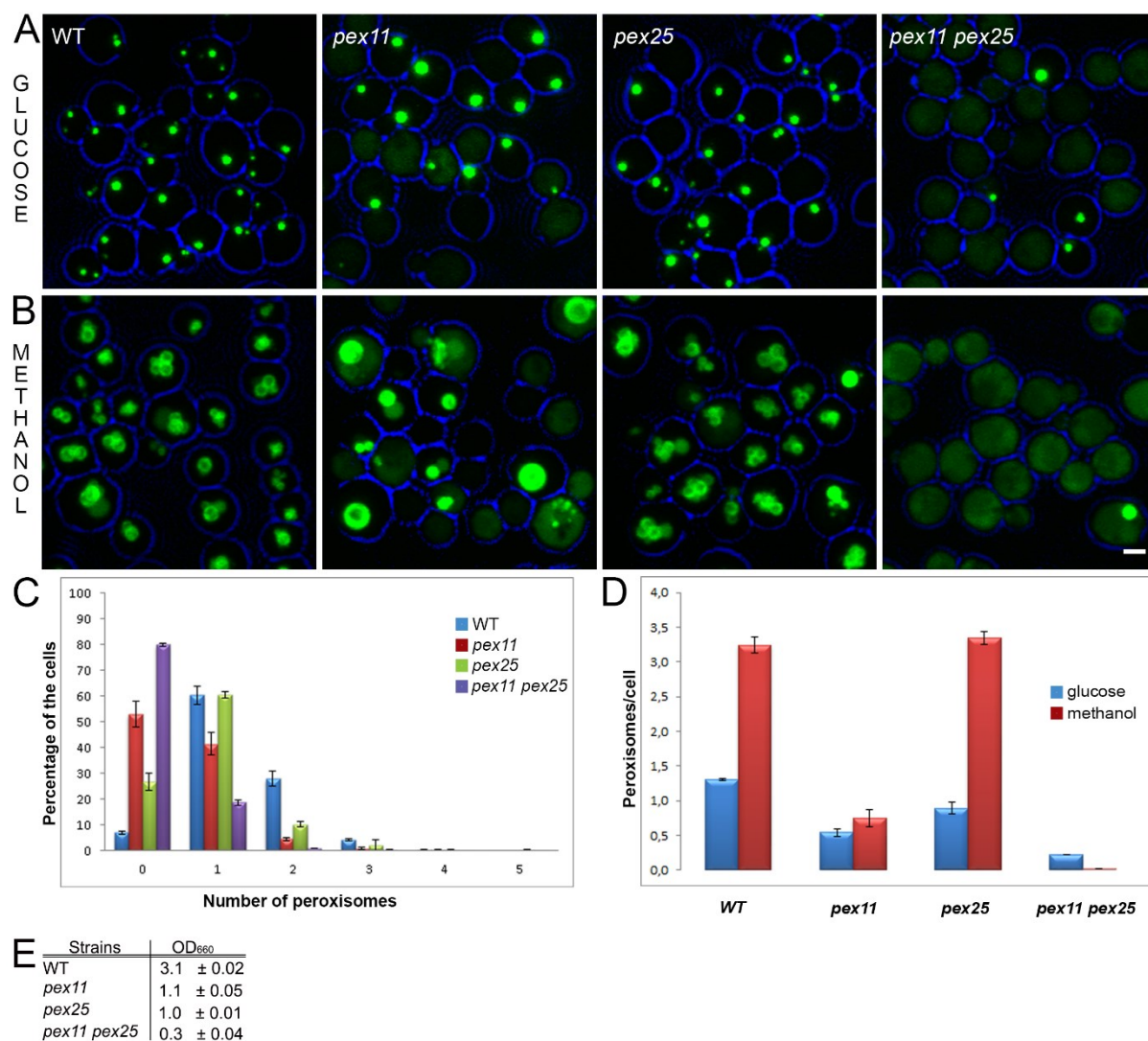


Figure 1. *pex11 pex25* cells show a severe reduction in peroxisome numbers. Intracellular localization of GFP-SKL in *H. polymorpha* WT, *pex11*, *pex25* and *pex11 pex25* cells producing GFP-SKL under control of the *TEF* (A) or *AOX* (B) promoter. Cells were grown for 4 hours on mineral medium containing glucose (MM-glu) (A) or for 16 hours on mineral medium containing methanol (MM/M) (B), respectively. FM images were obtained by CLSM. Bar=1 μ m. (C) Peroxisome number distribution of glucose grown cells. (D) Average peroxisome numbers per cell of cells grown on glucose or on methanol medium. (E) Optical densities of the indicated cultures upon growth for 16 h on methanol medium. For all peroxisome quantification data, average values were calculated from two biological replicates. 200 cells were counted manually per replicate. Error bars indicate standard deviation.

***pex11 pex25* cells harbor peroxisomal membrane structures**

Upon incubation on methanol medium, less than 1 % of the *pex11 pex25* cells have a peroxisome that imports GFP-SKL (**Fig. 1D**). In order to test whether PMP sorting is also affected, we introduced the peroxisomal membrane marker Pex14-GFP into these cells. As shown in **Fig 2A**, many but not all cells showed Pex14-GFP fluorescent spots, indicating that these cells contain peroxisomal membrane structures. To test whether the absence of Pex14 spots in some of the cells is due to autophagy, we deleted *ATG1* in *pex11 pex25* cells. As shown in **Fig. 2B**, all cells of this strain show Pex14-GFP spots, indicating that the spots are sensitive to autophagic degradation. This observation was confirmed by western blot analysis, which showed a reduction in Pex14 levels in *pex11 pex25* cells, which increased again upon deletion of *ATG1* (**Fig. 2E**). Quantification of Pex14 protein levels indicates that Pex14 protein levels in *pex11 pex25 atg1* cells nearly reached WT levels (**Fig. 2F**).

To analyze whether the Pex14-GFP spots in *pex11 pex25* cells represent clusters of membrane vesicles, we performed electron microscopy analysis. Immunolabelling experiments revealed that Pex14 is localized to small vesicular structures similar to those observed in other *pex11* double deletion strains (e.g. *pex11 vps13*, *pex11 ypt7*, *pex11 vps39*, chapters 2 and 3 this thesis) (**Fig. 2C**). These structures have a limited capacity to import matrix proteins. Hence, they most likely represent small peroxisomes. Indeed, immunolabelling experiments using anti-Pex3 antibodies showed that this peroxisomal membrane protein localizes to these structures as well (**Fig. 2D**).

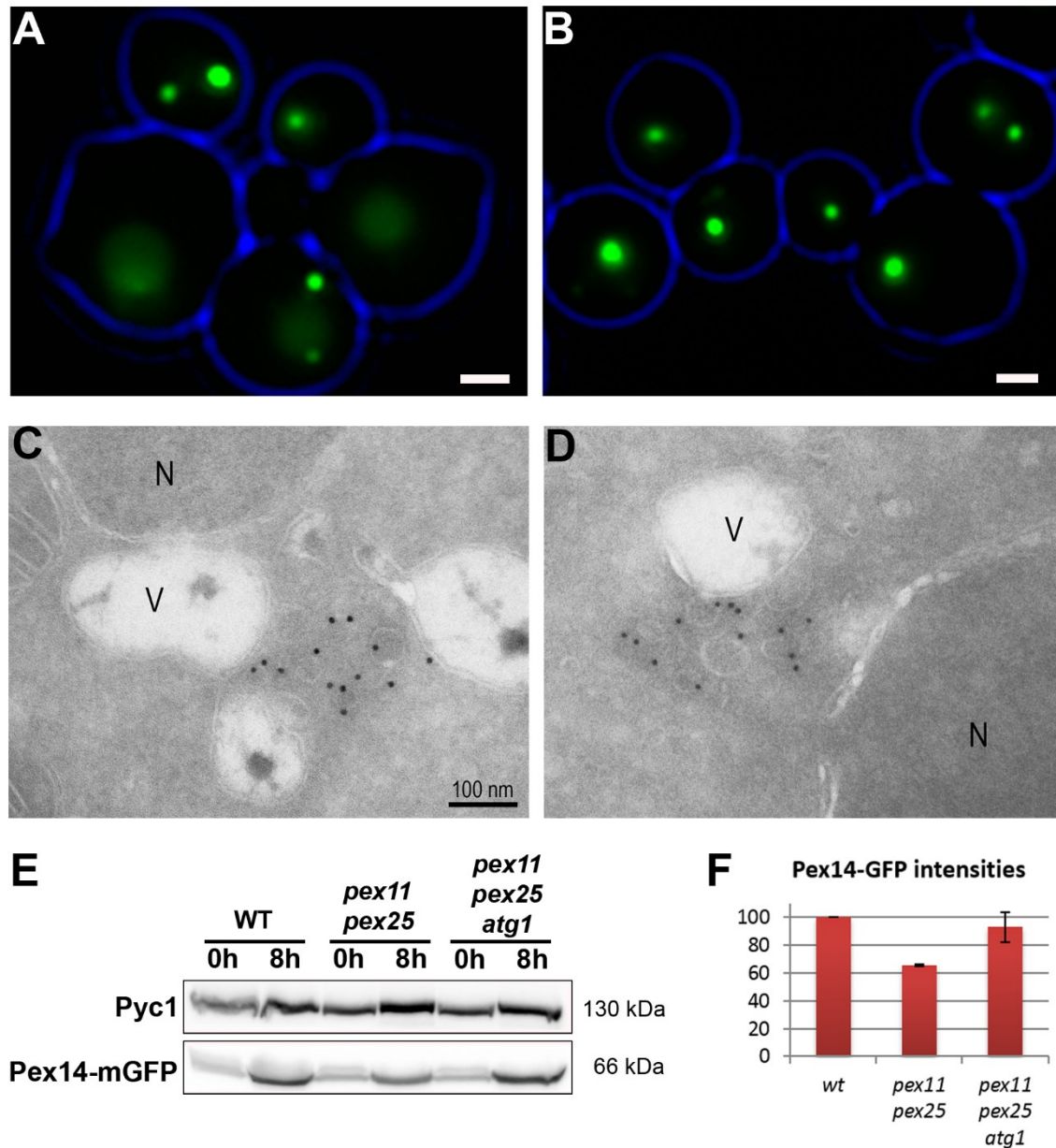


Figure 2. *pex11 pex25* cells harbor Pex14-containing structures. FM images of *pex11 pex25* (A) and of *pex11 pex25 atg1* (B) strains both producing Pex14-mGFP. Cells were grown for 8h on mineral medium containing methanol and glycerol (MM-M/G). Immuno-electron microscopy (iEM) analysis of *pex11 pex25 atg1* cells using α -Pex14 antibodies (C) or α -Pex3 antibodies (D) identifying clusters of membrane structures that are specifically labelled. N – nucleus; V - vacuole. (E) Western blot analysis of cells grown for 8h on MM-M/G using α -Pex14 antibodies. Pyruvate carboxylase (Pyc1) was used as a loading control. (F) Pex14-GFP levels were quantified using ImageJ software. Error bars represent SD based on 2 individual blots. Protein levels were corrected for Pyc1 levels and WT levels were set to 100%. Bars: (A,B) 1 μ m. (C,D) 100 nm.

Vesicles in *pex11 pex25* cells harbor certain PMPs

Next, we performed co-localization studies to analyze which additional PMPs were localized to the membrane structures (**Fig. 3**). This revealed that all peroxins tested (Pex3, Pex8, Pex13) co-localized with Pex14 on these structures (**Fig. 3A-C**).

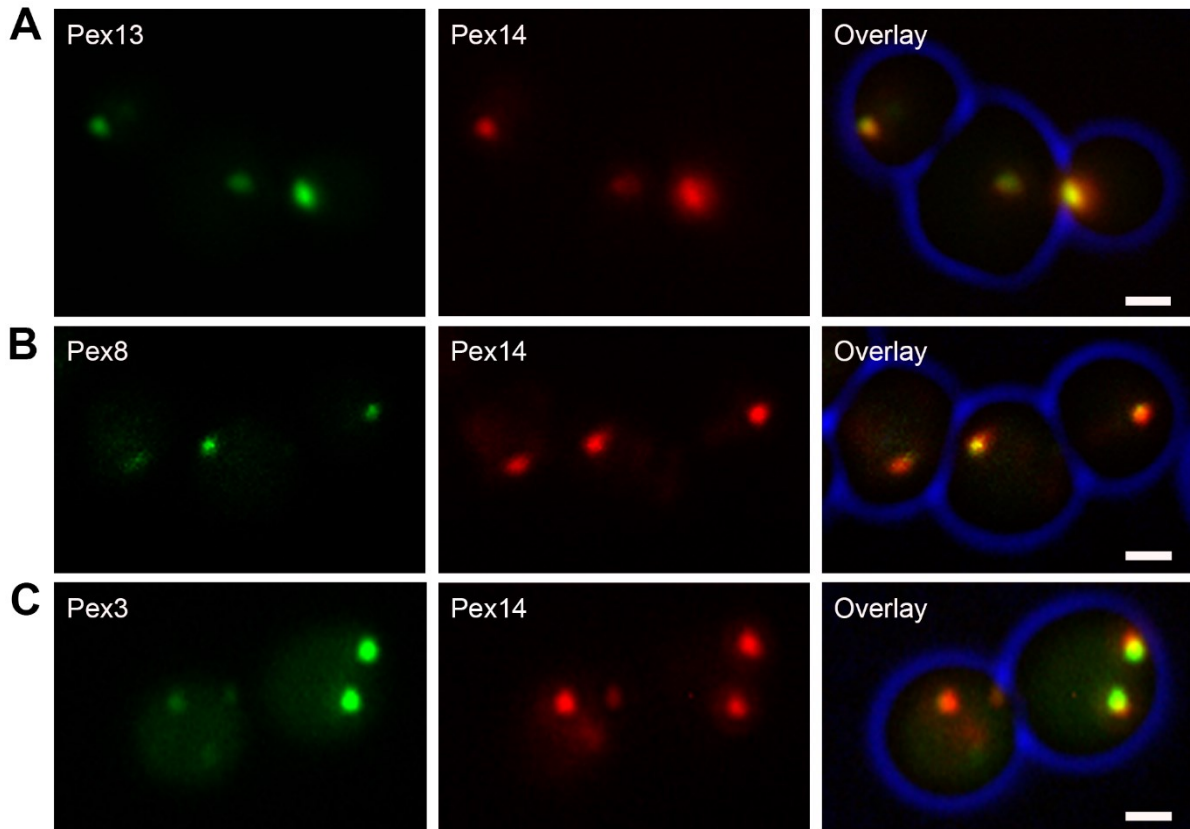


Figure 3. Localization of various PMPs in *pex11 pex25 atg1* cells. Fluorescence microscopy images of cells grown for 8h on MM-M/G. Cells produce Pex14-mCherry together with C-terminal mGFP fusions of the indicated proteins (A: Pex13, B: Pex8, C: Pex3). The scale bar indicates 1 μ m.

Pex14 containing structures in *pex11 pex25* cells mature into normal peroxisomes upon reintroduction of *PEX25*

In order to study whether the structures present in *pex11 pex25* cells can mature into normal peroxisomes, we constructed a *pex11 pex25* strain expressing *PEX25* under control of the inducible alcohol oxidase promoter (P_{AOX}) and also producing the peroxisomal membrane marker Pex14-mCherry as well as the matrix marker GFP-SKL. Cells were precultivated on glucose, to repress P_{AOX} and subsequently shifted to medium containing glycerol/methanol to induce P_{AOX} and peroxisome proliferation. After 60 min of incubation on glycerol/methanol medium, cytosolic GFP-SKL started to accumulate at the red fluorescent Pex14-mCherry spots, ultimately resulting in co-localization of all GFP with mCherry (after 90 min.) (**Fig. 4**).

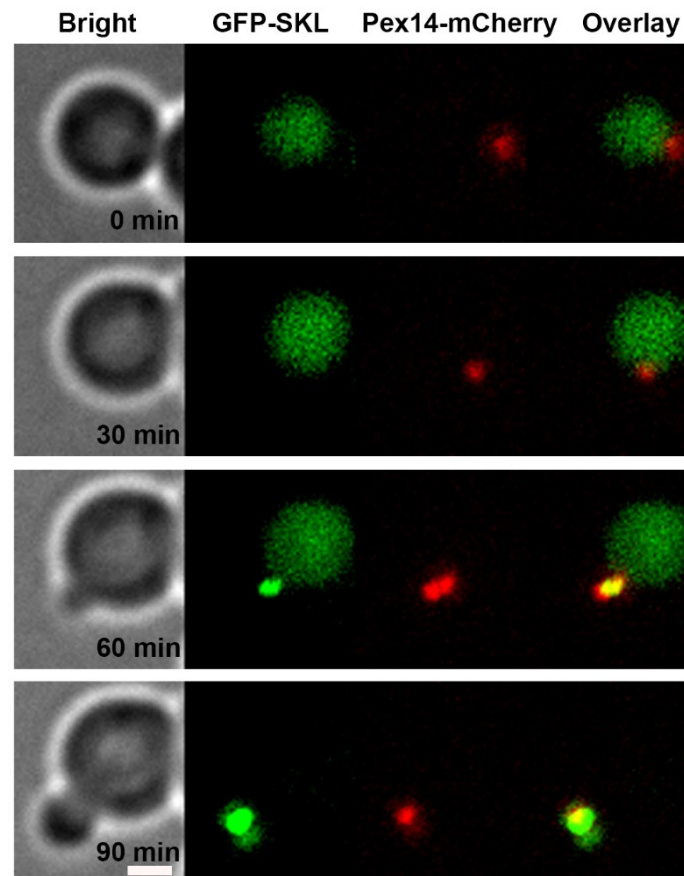


Figure 4. Pex14-containing membrane structures in *pex11 pex25* cells mature into peroxisomes upon reintroduction of Pex25. *pex11 pex25*. P_{AOX} Pex25 cells producing Pex14-mCherry and GFP-SKL pre-grown on glucose (0 min) were shifted to an agar slide supplemented with glycerol/methanol (0.05%/0.5% (v/v)) and followed in time by FM.

The re-introduced Pex25 sorted to the pre-existing Pex14-mCherry structures, as was evident from live cell imaging of a *pex11 pex25 atg1* strain producing Pex14-mCherry under the endogenous promoter and Pex25-mGFP under control of the inducible amine oxidase (*AMO*) promoter. After induction on glycerol/methanol/methylamine, the initial Pex25-mGFP fluorescence appeared on the Pex14-mCherry vesicles (**Fig. 5**) suggesting that the newly synthesized Pex25 directly sorts to these vesicles and peroxisomal structures mature into functional peroxisomes.

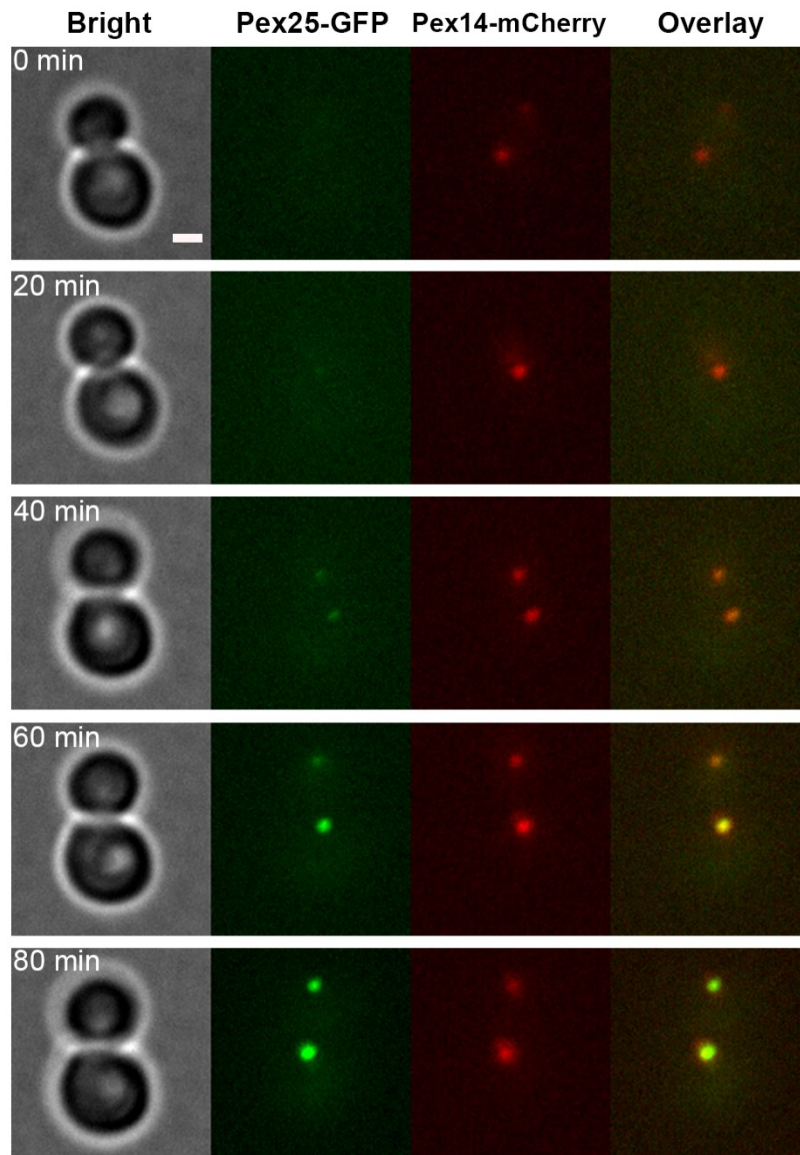


Figure 5. Upon reintroduction, Pex25 initially targets to the Pex14-containing structures. Live cell imaging of *pex11 pex25 atg1* cells producing Pex14-mCherry upon Pex25-GFP reintroduction after shifting cells from MM-glu with ammonium sulphate (0 min) to MM-M/G with methylamine. The scale bar is 1 μ m.

In addition, we did immune electron microscopy using Pex3 antibodies. 6h after reintroduction of Pex25 in *pex11 pex25* cells, multiple enlarged peroxisomal structures were observed. These peroxisomes were generally clustered and often located near the nucleus and vacuole (**Fig. 6**).

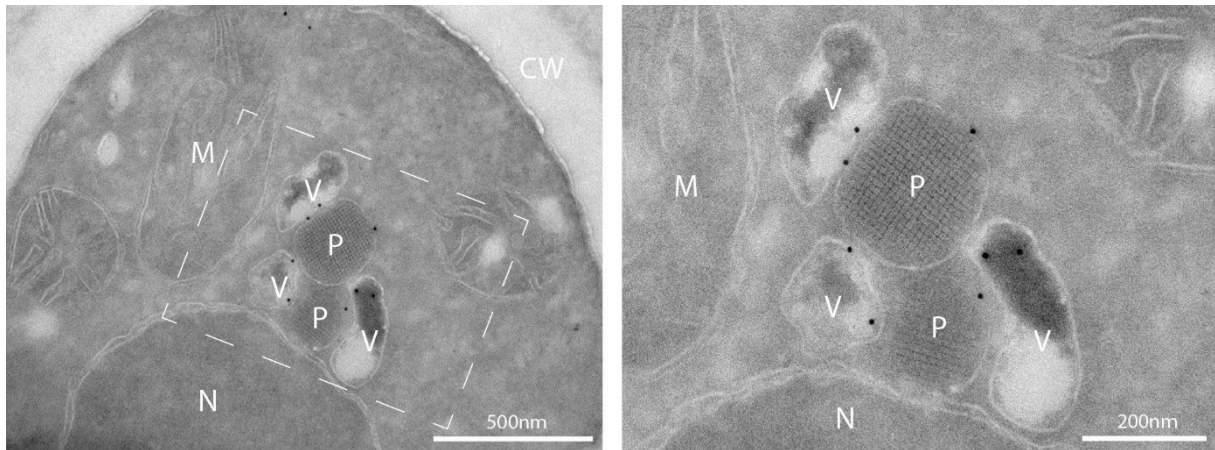


Figure 6. Pex25 reintroduction in *pex11 pex25* cells. iEM analysis of *pex11 pex25.PAOXPex25* cells using α -Pex3 antibodies. Cells were precultivated on MM-glu and induced for 6h on MM-M/G. Bars: 500 nm (left), 200 nm for the selection. CW – cell wall, M – mitochondrion, N – nucleus, P – peroxisome, V – vacuole.

The peroxisomal structures in *pex11 pex25* cells invariably are localized in the vicinity of fragmented vacuolar structures (**Fig. 2**) as observed in other double deletion mutants (i.e. *pex11 vps13*, *pex11 ypt7*, *pex11 vps39*) (Chapter 2 and 3, this thesis), whereas during reintroduction of Pex25 the peroxisomes seem to associate with vacuolar structures (**Fig. 6**). These observations point to possible defects in VAPCONS function in *pex11 pex25* cells that are restored upon Pex25 reintroduction.

To analyze whether Pex25 is indeed a possible VAPCONS component, we performed FM analysis of WT cells expressing Pex25-GFP and labelled with the vacuolar dye FM4-64. This revealed that Pex25-GFP localizes to the whole peroxisome membrane and sometimes is also found as spots. Interestingly, we also found that Pex25 occasionally forming a patch at the site of VAPCONS (**Fig. 7**).

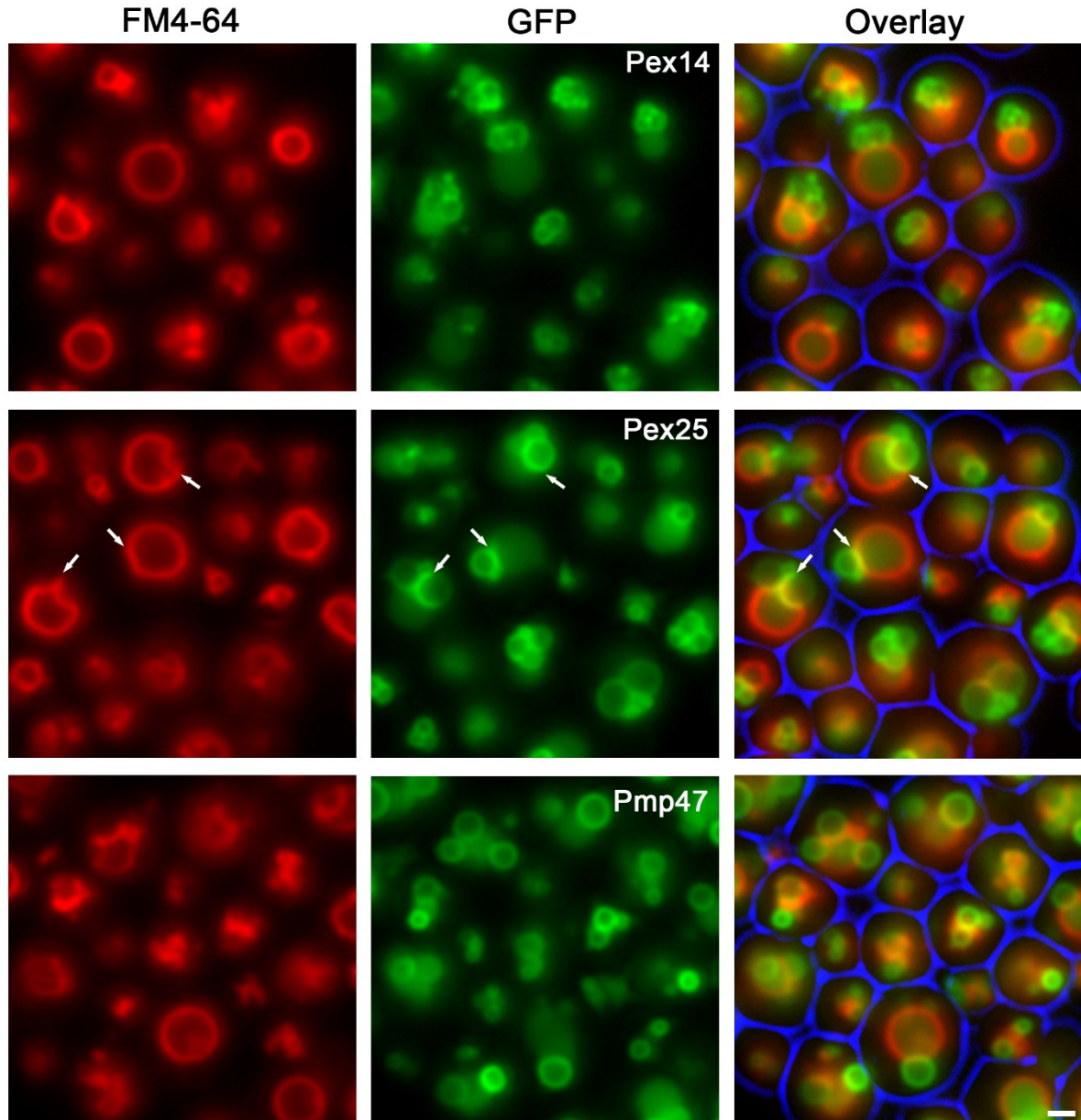


Figure 7. Pex25-GFP intensities are occasionally enhanced at VAPCONS. FM analysis of WT cells expressing C-terminal mGFP fusions of Pex14, Pex25 or PMP47 under control of their endogenous promoter. Cells were grown on MM/M for 16 hours and analyzed by FM. Vacuoles were labeled by FM4-64. Pex25-GFP concentration at the VAPCONS are indicated by white arrows. Scale bar: 1 μ m.

If Pex25 is important for VAPCONS formation, the absence of Pex25 may affect vacuolar morphology. FM analysis showed that in WT cells, peroxisomes are fully associated with vacuoles which show differing morphology (see also Chapter 3). We could easily detect peroxisome-vacuole associations also in *pex11* cells, though vacuoles surrounding (wrapping) peroxisomes were less abundant compared to WT cells. Interestingly, we observed enhanced peroxisome-vacuole associations in *pex25* cells, judged by the full colocalization of the peroxisomal membrane marker PMP47-GFP and the vacuolar marker FM4-64 (**Fig. 8**).

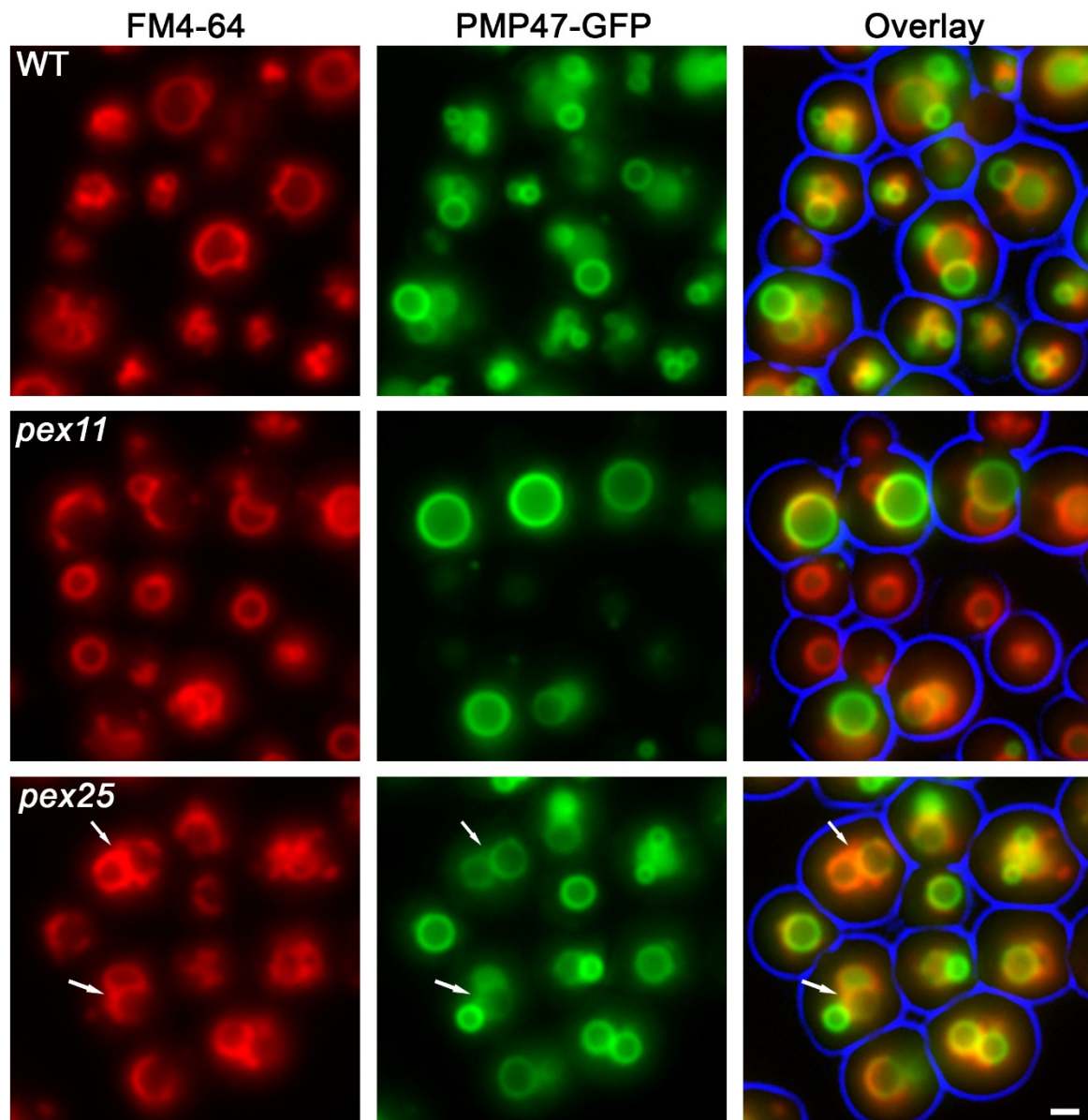


Figure 8. FM analysis of vacuole morphology in WT, *pex11* and *pex25*. Indicated strains expressing PMP47-GFP were grown on MM/M for 16h and analyzed by FM Axioskope. Vacuoles were labeled by FM4-64. Scale bar: 1 μ m.

Artificial link between PPVs and the ER results in peroxisome formation

pex11 vps13, *pex11 ypt7* and *pex11 vps39* mutants show similarities with *pex11 pex25* in that they contain small peroxisomal membrane structures (Chapter 2 and 3). The phenotype of these mutant strains could invariably be partially suppressed by the introduction of an ER-peroxisome tethering protein. Thus, we also introduced an artificial ER-peroxisome linker protein (Pex14-2*HA-Pho8^{N89}) in *pex11 pex25* cells. Our FM data showed that in the presence of the tether peroxisomes formed again for both conditions (**Fig. 9 A, C**).

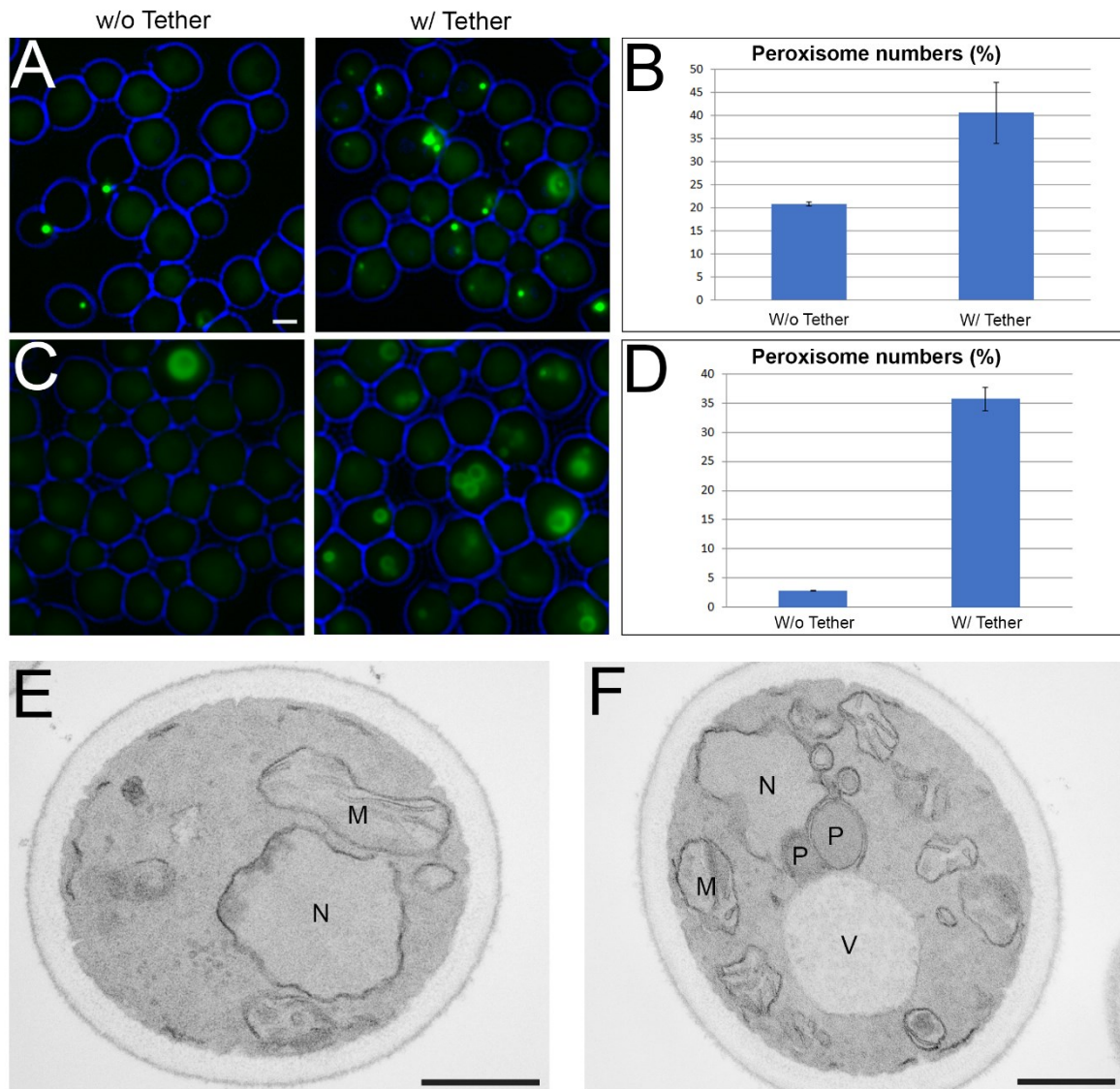


Figure 9. Artificial linker forms peroxisomes in *pex11 pex25 atg1* cells both on glucose and on glycerol/methanol. *pex11 pex25 atg1* cells producing GFP-SKL under TEF promoter and Pex14-2*HA-Pho8^{N89} under Adh1 promoter (right panel) were grown on MM-glu for 4 hours (A) or on MM-M/G for 16h (C). Scale bar is 1 μ m. Peroxisome number quantifications were made manually in duplo, ~500 cells were quantified for glucose (B) and glycerol/methanol cultures (D), respectively. EM analysis of *pex11 pex25 atg1* cells with (F) or w/o (E) artificial linker were shown. Cells were grown for 16h on MM/G-M. N=Nucleus; M=Mitochondrion; V=Vacuole; P=Peroxisome. Scale bar is 500 nm.

EM analysis confirmed that the linker protein indeed associated the ER to peroxisomes (Fig. 9 F). It is clear that peroxisomes are surrounded by the ER. Quantification of peroxisome numbers showed a significant increase in the numbers of peroxisomes (Fig. 9 B, D).

Discussion

In this study, we show that *H. polymorpha pex11 pex25* cells are indeed peroxisome deficient as suggested by a previous mutagenesis screen (Chapter 2, this thesis). Even though cells of *pex11* and *pex25* single deletion strains contain functional peroxisomes, these organelles are absent in *pex11 pex25* cells when grown on medium which requires proliferation of the peroxisomes (methanol; **Fig. 1**). This observation is in line with data obtained for *S. cerevisiae*, which revealed that deletion of *PEX11* in *pex25* cells disturbed fatty-acid utilization, which requires functional peroxisomes as well (Rottensteiner et al., 2003).

Our data indicated that cells of a *H. polymorpha pex25* single deletion strain show reduced growth on methanol, which is similar to that of *Hp pex11* cells, though *pex25* cells are not affected in terms of peroxisome numbers (**Fig. 1**).

Our finding that cells of a *pex11 pex25* double deletion strain are unable to grow on methanol and contain small peroxisomes together with the mislocalisation of matrix proteins suggests that both Pex11 and Pex25 play a role in peroxisome growth (**Fig. 1**). These small peroxisomes contained all PMPs tested, namely Pex3, Pex8, Pex13 and Pex14, and morphologically resembled peroxisomal structures present in *pex11 ypt7*, *pex11 ups13*, *pex23 ypt7*, *pex23 ups13*, *pex24 ypt7*, *pex24 ups13* cells (**Fig. 2 CD**; Chapter 2, 3 this thesis). Similar as observed in *pex11 ypt7* cells (**Fig. 5C**, Chapter 3 this thesis), the small peroxisomes harboured a minor portion of peroxisomal matrix protein. Hence they do contain a functional importomer. Therefore, the lack of complete import of all matrix protein is most likely due to a defect in the growth of the organelles indirectly leading to mislocalisation of the bulk of the matrix proteins. We analyzed whether the peroxisomes already present in *pex11 pex25* cells can grow upon re-introduction of Pex25. This revealed that Pex25 initially sorted to the already-existing peroxisomes, which matured into functional peroxisomes capable of fully importing matrix proteins. This further supports the view that peroxisome membrane growth is blocked in *pex11 pex25* cells and restored upon Pex25 reintroduction (**Fig. 4-6**).

Previous data suggested that in *H. polymorpha* peroxisome-vacuole associations are important for the expansion of the peroxisome membrane under peroxisome proliferation conditions (Chapter 3). Our EM data showed that upon reintroduction of *PEX25* in *pex11 pex25* cells, newly formed peroxisomes appear in the vicinity of vacuoles and nucleus (**Fig. 6**). Moreover, at some peroxisomes Pex25-GFP is present at slightly higher levels at VAPCONS compared to other regions of the organelle (**Fig. 7**). Interestingly, peroxisomes in *pex25* cells are fully enwrapped by vacuoles (**Fig. 8**), indicating that Pex25 is not essential for the formation of VAPCONS. As VAPCONS are still present in *pex25* cells, Pex25 might be a negative regulator of this contact.

It should be noted that increased peroxisome-vacuole associations in *pex25* cells might limit lipid transport from other membrane sources (i.e. the ER, plasma membrane, mitochondria) and change the lipid composition of the peroxisomal membrane. Possibly this explains the reduced growth of *pex25* cells on methanol, despite the fact that peroxisomes are normally present. Whether the enhanced peroxisome-vacuole associations in *pex25* cells are caused by increased expression of other VAPCONS components need further investigation. Another possibility for enhanced peroxisome-vacuole contacts might be also related to other functions of Pex25. It was demonstrated that in *S. cerevisiae* the small GTPase Rho1, which is mainly localized to the plasma membrane, is recruited to the peroxisome membrane via interaction with Pex25. At this location it regulates peroxisome dynamics by assembling actin on the peroxisome membrane (Marelli et al., 2004; Logan et al., 2010). Interestingly, data have been presented that Rho1 also functions in regulating vacuole membrane fusion (Logan et al., 2010). Hence, it is tempting to speculate that Rho1 also may regulate peroxisome/vacuole contacts.

As Pex25 is localized at the entire peroxisome surface, we cannot rule out that it might also play a role in peroxisome associations with the ER. It was shown that peroxisomes in *S. cerevisiae* are tethered to the ER by both Pex3-Inp1 and Pex30, which function in peroxisome inheritance and *de novo* peroxisome biogenesis, respectively (Knoblach et al., 2013; Mast et al., 2016; David et al., 2013). Interestingly Inp1, which regulates peroxisome retention in the mother cell, interacts both with Pex30 and Pex25 (Fagarasanu et al., 2005) suggesting that the loss of Pex25 from the peroxisome membrane might decrease lipid supply from the ER, which could result in enhancement of VAPCONS.

In order to test whether the observed defect of *pex11 pex25* is related to ER membrane contact sites (MCS), we produced an artificial linker protein in these cells, which links peroxisomes to the ER. Our data show that peroxisomes were formed again in these cells upon artificial tethering to the ER (**Fig. 9**). Our findings suggest that peroxisomal membrane structures are present in *pex11 pex25* cells that may be unable to grow due to defects in both EPCONS (caused by *PEX11* deletion) and VAPCONS (caused by *PEX25* deletion).

Materials and methods

Strains and growth conditions

H. polymorpha strains used in this study are listed in **Table 1**. Yeast cultures were grown at 37°C on (a) YPD media containing 1% yeast extract, 1% peptone, and 1% glucose; or (b) mineral media (MM; van Dijken et al., 1976) supplemented with 0.5% glucose, or 0.5% methanol as carbon source eventually supplemented with 0.05% glycerol. Leucine was added to a final concentration of 30 µg/ml. For growth on agar plates the medium was supplemented with 2% agar. For the selection of resistant transformants, YPD plates containing 200 µg/ml zeocin or 300 µg/ml hygromycin (Invitrogen) were used.

For cloning purposes, *E. coli* DH5alpha was used. Cells were grown at 37°C in LB media supplemented with 100 µg/ml ampicillin or 25 µg/ml zeocin when required. Cells were grown in shake flask cultures as described previously (Knoops et al., 2014).

Molecular Techniques

Plasmids and primers used in this study are listed in **Table 2** and **3**, respectively. Recombinant DNA manipulations and transformations of *H. polymorpha* were performed as described before (Faber et al., 1994). Preparative polymerase chain reactions (PCR) for cloning were carried out with Phusion High-Fidelity DNA Polymerase (Thermo Scientific). Initial selection of positive transformants by colony PCR was carried out using Phire polymerase (Thermo Scientific). All deletions were confirmed by Southern blotting. For DNA and amino acid sequence analysis, the Clone Manager 5 program (Scientific and Educational Software, Durham, NC.) was used.

Construction of *H. polymorpha* *pex25* and *pex11 pex25* strains

Two plasmids allowing disruption of *H. polymorpha* *PEX25* were constructed using Multisite Gateway technology as follows: First, the 5' and 3' flanking regions of the *PEX25* gene were amplified by PCR with primers RSAPex25-1+RSAPex25-2 and RSAPex25-3+RSAPex25-4, respectively, using *H. polymorpha* NCYC495 genomic DNA as a template. The resulting fragments were then recombined in donor vectors pDONR P4-P1R and pDONR P2R-P3, resulting in plasmids pENTR-PEX25 5' and pENTR-PEX25 3', respectively. Then, PCR amplification was performed using primers attB1-Ptef1-forward and attB2-Ttef1-reverse using pHIPN4 as the template. The resulting PCR fragment was recombined into vector pDONR-221 yielding entry vector pENTR-221-NAT. Recombination of the entry vectors pENTR-PEX25 5', pENTR-221-NAT, and pENTR-PEX25 3', and the destination vector pDEST-R4-R3, resulted in

pRSA018. Then *PEX25* disruption cassette containing neomycin resistance gene was amplified with primers RSAPex25-5 and RSAPex25-6 using pRSA018 as a template.

To create *pex25* and *pex11 pex25* strains, the *PEX25* disruption cassette was transformed into *yku80* and *pex11* cells, respectively. Correct deletions were confirmed by cPCR and southern blot analysis.

Construction of *H. polymorpha* WT GFP-SKL, *pex11* GFP-SKL, *pex25* GFP-SKL and *pex11 pex25* strains

To create strains for FM quantification analysis, *StuI*-linearized pHIPX7-GFP-SKL or *StuI*-linearized pHIPX4-GFP-SKL was transformed into WT, *pex11*, *pex25* and *pex11 pex25* cells.

Construction of *H. polymorpha* WT *PEX14*-GFP and *pex11 pex25 PEX14*-GFP strains

To create WT *PEX14*-GFP and *pex11 pex25 PEX14*-GFP strains, *PstI*-linearized pSNA12 was transformed into WT and *pex11 pex25* cells. Zeocin resistant transformants were selected and checked by colony PCR using primers Pex14FWD and R-GFP.

Construction of *H. polymorpha pex11 pex25 atg1 PEX14*-GFP, *pex5 atg1 PEX14*-GFP strains and the strains for co-localization studies

Two plasmids allowing disruption of *H. polymorpha ATG1* were constructed using Multisite Gateway technology as follows. First, the 5' and 3' flanking regions of the *ATG1* gene were amplified by PCR with primers ATG1_5'_fwd+ATG1_5'_rev and ATG1_3'_fwd+ATG1_3'_rev, respectively, using *H. polymorpha* NCYC495 genomic DNA as a template. The resulting fragments were then recombined in vectors pDONR P4-P1R and pDONR P2R-P3, resulting in plasmids pENTR ATG1 5' and pENTR ATG1 3', respectively. Both entry plasmids were recombined with destination vector pDEST R4-R3 together with entry plasmid pENTR221-hph, resulting in plasmid pARM011 (pDEL ATG1). Then, deletion cassette was amplified with primers pDEL_ATG1_fwd and pDEL_ATG1_rev, using pARM011 as a template.

To create *pex11 pex25 atg1* strain, the *ATG1* disruption cassette containing the hygromycin resistance gene was transformed into *pex11 pex25* cells and hygromycin resistant transformants were selected and checked by colony PCR using primers ATG1_cPCR_fwd and ATG1_cPCR_rev. Correct disruptions were confirmed by colony PCR and southern blotting. Finally, *PstI*-linearized pSNA12

was transformed into *pex11 pex25 atg1* which resulted in *pex11 pex25 atg1 PEX14-GFP*.

For co-localization analysis, first a plasmid encoding Pex14 with a C-terminal mCherry fluorescent protein was constructed as follows: First, a PCR fragment containing Pex14-mCherry was amplified with primers PRARM001 and PRARM002 using pSEM01 as a template. The obtained PCR fragment was digested with *NotI* and *HindIII*, and inserted between the *NotI* and *HindIII* sites of plasmid pHIPX7, resulting in plasmid pARM014 (pHIPX-*PEX14*-mCherry). *BlnI*-linearized pARM014 was transformed into *pex11 pex25 atg1* cells, which resulted in *pex11 pex25 atg1 PEX14*-mCherry. Then, pHIPZ-*PEX3*-mGFP, pMCE4 and pSEM03 were linearized by *EcoRI*, *EcoRI* and *ApaI*, respectively, and transformed into *pex11 pex25 atg1 PEX14*-mCherry cells. Correct integrations were confirmed by colony PCR.

Construction of *H. polymorpha pex11 pex25* P_{AOX}*PEX25 PEX14*-mCherry GFP-SKL

A plasmid expressing *PEX25* under the control of inducible alcohol oxidase promoter (P_{AOX}) was constructed as follows: First, a 519 bp *Bam*HI–*Nco*I fragment from pREMI-Z was inserted between the *Bam*HI and *Nco*I of pHIPZ4-Nia to get plasmid pDEST-Zeo-tussen. The 1143 bp *Hind*III–*Asp*718I fragment (blunted) from pDEST-Zeo-tussen was ligated with pDEST-R4-R3 (digested with *Sfo*I) which resulted in pRSA07. To construct pRSA08, following plasmids were constructed: pRSA01, pRSA02, pENTR-P4-P1R-P_{AOX} and pENTR-221-*PEX25*. For the construction of plasmid pRSA01, a PCR fragment of 700 bp was obtained by primers RSA10fw and RSA11rev on pCDNA3.1mCherry. The resulting *Bgl*II–*Sal*I fragment was inserted between the *Bgl*II and *Sal*I of pANL31. For construction of plasmid pRSA02, PCR was done with primers RSA12Fw and RSA13Rev on pRSA01. The PCR fragment was cloned into the vector pDONR-P2R-P3, resulting in the entry vector pRSA02. For the construction of entry vector pENTR-P4-P1R-P_{AOX}, PCR amplification was done with primers *att* P_{AOX} F and *att* P_{AOX} R on pANL29. The PCR fragment was cloned in entry vector pDONR-P4-P1R resulting in the entry vector pENTR-P4-P1R-P_{AOX}. The *PEX25* coding sequence lacking a stop codon was amplified using the primers BB-JK-037 and BB-JK-038 and cloned into the vector pDONR-221 resulting in plasmid pENTR-221-*PEX25*. pRSA08 was obtained by recombination of pENTR-P4-P1R-P_{AOX}, pENTR-221-*PEX25*, and pRSA02 and destination vector pRSA07. Next, the *PEX25* gene was amplified with primers AOX_StuI_fwd and Pex25_SalI_rev using pRSA08 as a template. The obtained fragment and plasmid pHIPH4 were cut with *Sal*I and *Stu*I, and ligated with each other, resulting in plasmid pARM026 (pHIPH4-*PEX25*). Then, the *Stu*I linearized pARM026 was transformed into *pex11 pex25* cells, resulting in *pex11 pex25* P_{AOX}*PEX25*. Correct

integrations were checked by AOX_up_fwd+Pex25_cPCR_rev. To create a *pex11 pex25* P_{AOX}PEX25 PEX14-mCherry strain, first *BlpI*-linearized pARM014 was transformed into *pex11 pex25* P_{AOX}PEX25 cells. Then, *MunI*-linearized pAKW27 was transformed into *pex11 pex25* P_{AOX}PEX25 PEX14-mCherry strain, which resulted in *pex11 pex25* P_{AOX}PEX25 PEX14-mCherry GFP-SKL.

Construction of *H. polymorpha pex11 pex25 atg1* PEX14-mCherry P_{AMO}PEX25-GFP

A plasmid encoding *Hansenula polymorpha* Pex25 with a C-terminal monomeric green fluorescent protein (mGFP) under the control of inducible amine oxidase promoter (P_{AMO}) was constructed using Multisite Gateway technology as follows: The plasmids pRSA07, pENTR-221-PEX25, pENTR23-mGFP-T_{AMO} and pENTR41-P_{AMO} were recombined resulting in pARM027 (pHIPZ5-PEX25-mGFP). Finally, *EheI*-linearized pARM027 was transformed into *pex11 pex25 atg1* PEX14-mCherry cells. Correct integrations were checked by AMO_sel_f and mGFP_rev_check.

Construction of *H. polymorpha* WT PEX25-mGFP

To create WT Pex25-mGFP, *PstI*-linearized pMCE1 was transformed into *yku80* strain. Correct integrations were checked by Pex25_cPCR_fwd+mGFP_rev_check.

Construction of *H. polymorpha pex11 pex25 atg1* strain with an artificial ER linker

To create pARM032 (pHIPZ18-PEX14-2xHA-PHO8^{N89}), PCR fragments PEX14-2xHA and 2xHA-PHO8^{N89} were amplified by primers *HindIII*-Pex14+Pex14_HA-HA and HA-HA_Ph08+Pho8_PspXI (2), respectively using the *H. polymorpha* NCYC 495 genomic DNA as a template. The obtained PCR fragments were purified and used as templates together with primers *HindIII*-Pex14+Pho8_PspXI_rev (2) in a second PCR reaction. The obtained PCR fragment was digested with *HindIII* and *PspXI*, and inserted between the *HindIII* and *SalI* sites of pAMK94 plasmid, resulting in plasmid pARM032. Then, the *NruI*-linearized pARM032 was transformed into *pex11 pex25 atg1* cells. Correct integrations were confirmed by colony PCR with primers Adh1_cPCR_fwd+Pho8_cPCR_rev. Finally, *BciVI*-linearized pHIPX7-GFP-SKL was transformed into these cells, which resulted in *pex11 pex25 atg1* P_{ADH1}-PEX14-2xHA-PHO8^{N89} GFP-SKL.

Table 1. *H. polymorpha* strains used in this study

Strains	Description	References
WT	NCYC495, <i>leu 1.1</i>	(Gleeson and Sudbery, 1988)
<i>pex11</i>	<i>PEX11::URA3</i>	(Krikken et al., 2009)
<i>pex25</i>	<i>PEX25::NAT YKU80::URA3</i>	This study
<i>pex11 pex25</i>	<i>PEX11::URA3 PEX25::NAT</i>	This study
WT GFP-SKL	pHIPX7-GFP-SKL:: <i>LEU2</i>	This study
<i>pex11</i> GFP-SKL	<i>PEX11::URA3</i> pHIPX7-GFP-SKL:: <i>LEU2</i>	This study
<i>pex25</i> GFP-SKL	<i>PEX25::NAT YKU80::URA3</i> pHIPX7-GFP-SKL:: <i>LEU2</i>	This study
<i>pex11 pex25</i> GFP-SKL	<i>PEX11::URA3 PEX25::NAT</i> pHIPX7-GFP-SKL:: <i>LEU2</i>	This study
WT P _{AOX} GFP-SKL	pHIPX4-GFP-SKL:: <i>LEU2</i>	This study
<i>pex11</i> P _{AOX} GFP-SKL	<i>PEX11::URA3</i> pHIPX4-GFP-SKL:: <i>LEU2</i>	This study
<i>pex25</i> P _{AOX} GFP-SKL	<i>PEX25::NAT YKU80::URA3</i> pHIPX4-GFP-SKL:: <i>LEU2</i>	This study
<i>pex11 pex25</i> P _{AOX} GFP-SKL	<i>PEX11::URA3 PEX25::NAT</i> pHIPX4-GFP-SKL:: <i>LEU2</i>	This study
WT <i>PEX14</i> -mGFP	pSNA12:: <i>sh ble</i>	(Knoops et al., 2014)
<i>pex11 pex25 PEX14</i> -mGFP	<i>PEX11::URA3 PEX25::NAT</i> pSNA12:: <i>sh ble</i>	This study
<i>pex11 pex25 atg1</i>	<i>PEX11::URA3 PEX25::NAT ATG1::HPH</i>	This study
<i>pex11 pex25 atg1 PEX14</i> -mGFP	<i>PEX11::URA3 PEX25::NAT ATG1::HPH</i> pSNA12:: <i>sh ble</i>	This study
<i>pex11 pex25 atg1 PEX14</i> -mCherry	<i>PEX11::URA3 PEX25::NAT ATG1::HPH</i> pARM014:: <i>LEU2</i>	This study
<i>pex11 pex25 atg1 PEX14</i> -mCherry <i>PEX3</i> -mGFP	<i>PEX11::URA3 PEX25::NAT ATG1::HPH</i> pARM014:: <i>LEU2</i> pHIPZ- <i>PEX3</i> -mGFP:: <i>sh ble</i>	This study
<i>pex11 pex25 atg1 PEX14</i> -mCherry <i>PEX8</i> -mGFP	<i>PEX11::URA3 PEX25::NAT ATG1::HPH</i> pARM014:: <i>LEU2</i> pMCE4:: <i>sh ble</i>	This study
<i>pex11 pex25 atg1 PEX14</i> -mCherry <i>PEX13</i> -mGFP	<i>PEX11::URA3 PEX25::NAT ATG1::HPH</i> pARM014:: <i>LEU2</i> pSEM03:: <i>sh ble</i>	This study
<i>pex11 pex25</i> P _{AOX} <i>PEX25</i>	<i>PEX11::URA3 PEX25::NAT</i> pARM026:: <i>HPH</i>	This study
<i>pex11 pex25</i> P _{AOX} <i>PEX25 PEX14</i> -mCherry	<i>PEX11::URA3 PEX25::NAT</i> pARM026:: <i>HPH</i> pARM014:: <i>LEU2</i>	This study
<i>pex11 pex25</i> P _{AOX} <i>PEX25 PEX14</i> -mCherry GFP-	<i>PEX11::URA3 PEX25::NAT</i> pARM026:: <i>HPH</i> pARM014:: <i>LEU2</i>	This study

SKL	pAKW27:: <i>sh ble</i>	
<i>pex11 pex25 atg1</i> <i>PEX14</i> -mCherry P _{AMO} <i>PEX25</i> -mGFP	<i>PEX11::URA3 PEX25::NAT ATG1::HPH</i> pARM014:: <i>LEU2</i> pARM027:: <i>sh ble</i>	This study
WT <i>PEX25</i> -mGFP	pMCE1:: <i>sh ble YKU80::URA3</i>	This study
<i>pex11 pex25 atg1</i> P _{ADH1} <i>PEX14</i> -2HA- <i>PHO8^{N89}</i>	<i>PEX11::URA3 PEX25::NAT ATG1::HPH</i> pARM032:: <i>sh ble</i>	This study
<i>pex11 pex25 atg1</i> P _{ADH1} <i>PEX14</i> -2HA- <i>PHO8^{N89}</i> GFP-SKL	<i>PEX11::URA3 PEX25::NAT ATG1::HPH</i> pARM032:: <i>sh ble</i> pHIPX7-GFP- SKL:: <i>LEU2</i>	This study

Table 2. Plasmids used in this study

Plasmids	Description	References
pDONR P4-P1R	Multisite Gateway vector; Kan ^R , Cm ^R	Invitrogen
pDONR P2R-P3	Multisite Gateway vector; Kan ^R , Cm ^R	Invitrogen
pENTR <i>PEX25</i> 5'	pDONR P4-P1R with 5' flanking region of <i>PEX25</i> ; Kan ^R	This study
pENTR <i>PEX25</i> 3'	pDONR P2R-P3 with 3' flanking region of <i>PEX25</i> ; Kan ^R	This study
pHIPN4	pHIPN plasmid containing AOX promoter; Nat ^R , Amp ^R	(Cepińska et al., 2011)
pDONR-221	Multisite gateway donor vector; Kan ^R , Cm ^R	Invitrogen
pENTR-221-NAT	pDONR 221 with <i>NAT</i> cassette; Nat ^R , Kan ^R	This study
pDEST-R4-R3	Multisite Gateway donor vector; Amp ^R , Cm ^R	Invitrogen
pRSA018	Plasmid containing <i>PEX25</i> deletion cassette; Zeo ^R , Amp ^R	This study
pHIPX7-GFP-SKL	pHIPX plasmid containing GFP-SKL under the control of P _{TEF1} ; <i>LEU2</i> , Kan ^R	(Baerends et al., 1997)
pHIPX4-GFP-SKL	pHIPX plasmid containing GFP-SKL under the control of P _{AOX} ; <i>LEU2</i> , Kan ^R	(Faber et al., 2002)
pSNA12	pHIPZ plasmid containing gene encoding C-terminal of Pex14 fused to mGFP; Zeo ^R , Amp ^R	(Cepińska et al., 2011)
pENTR <i>ATG1</i> 5'	pDONR P4-P1R with 5' flanking region of <i>ATG1</i> ; Kan ^R	This study
pENTR <i>ATG1</i> 3'	pDONR P2R-P3 with 3' flanking region of <i>ATG1</i> ; Kan ^R	This study
pENTR221-hph	pDONR 221 with <i>HPH</i> ; Hph ^R , Kan ^R	(Saraya et al., 2012)
pARM011	Plasmid containing <i>ATG1</i> deletion cassette; Hph ^R , Amp ^R	This study
pSEM01	pHIPN plasmid containing gene encoding C-terminal of Pex14 fused to mCherry; Nat ^R , Amp ^R	(Knoops et al., 2014)
pHIPX7	pHIPX plasmid containing TEF1 promoter; <i>LEU2</i> , Kan ^R	(Baerends et al., 1996)
pARM014	pHIPX plasmid containing gene encoding C-terminal of Pex14 fused to mCherry; <i>LEU2</i> , Kan ^R	This study
pHIPZ- <i>PEX3</i> -mGFP	pHIPZ plasmid containing gene encoding C-terminal of Pex3 fused to mGFP; Zeo ^R , Amp ^R	Chapter 2
pMCE4	pHIPZ plasmid containing gene encoding C-terminal of Pex8 fused to mGFP; Zeo ^R ,	(Cepińska et al., 2011)

	Amp ^R	
pSEM03	pHIPZ plasmid containing gene encoding C-terminal of Pex13 fused to mGFP; Zeo ^R , Amp ^R	(Knoops et al., 2014)
pREMI-Z	REMI plasmid; Zeo ^R , Amp ^R	(van Dijk et al., 2001)
pHIPZ4-Nia	pHIP plasmid containing Nia under AOX promoter; Zeo ^R , Amp ^R	(Faber et al., 2001)
pDEST-Zeo-tussen	pDEST with Zeocin marker; Zeo ^R , Amp ^R	This study
pRSA07	pDEST-R4-R3 containing zeocin marker; Zeo ^R , Amp ^R	This study
pCDNA3.1mCherry	Plasmid containing mCherry; Amp ^R	(Shaner et al., 2004)
pANL31	pHIP containing eGFP fusinator; Amp ^R , Zeo ^R	(Leão-Helder et al., 2003)
pRSA01	pHIP containing mCherry fusinator under AOX promoter; Zeo ^R	This study
pRSA02	pDONR-P2R-P3 containing mCherry-T _{AMO} , Kan ^R	This study
pANL29	pHIP containing GFP-SKL under AOX promoter; Zeo ^R , Amp ^R	(Leão-Helder et al., 2003)
pENTR-P4-P1R-P _{AOX}	pDONR-P4-P1R containing AOX promoter, Kan ^R	This study
pENTR-221- <i>PEX25</i>	Gateway entry clone containing <i>PEX25</i> without stop codon, Kan ^R	This study
pRSA08	pHIP plasmid containing gene encoding Pex25 fused to mCherry under AOX promoter; Zeo ^R , Amp ^R	This study
pHIPH4	pHIPH plasmid containing AOX promoter; Hph ^R , Amp ^R	(Saraya et al., 2012)
pARM026	pHIPH plasmid containing <i>PEX25</i> under the control of P _{AOX} ; Hph ^R , Amp ^R	This study
pAKW27	pHIPZ plasmid containing GFP-SKL under the control of P _{TEF1} ; Zeo ^R , Amp ^R	(Knoops et al., 2014)
pDONR-221	Multisite gateway donor vector; Kan ^R , Cm ^R	Invitrogen
pENTR23-mGFP-T _{AMO}	pDONR P2R-P3 with mGFP-T _{AMO} ; Kan ^R	(Nagotu et al., 2008a)
pENTR41-P _{AMO}	pDONR P4-P1R with P _{AMO} ; Kan ^R	Laboratory collection
pARM027	pHIP plasmid containing <i>PEX25</i> -mGFP under the control of P _{AMO} ; Zeo ^R , Amp ^R	This study
pMCE1	pHIPZ plasmid containing gene encoding C-terminal of Pex25 fused to mGFP; Zeo ^R , Amp ^R	(Cepińska et al., 2011)
pAMK94	pHIPZ plasmid containing GFP-SKL under	Chapter 2

	the control of P_{ADH1} ; Zeo ^R , Amp ^R	
pARM032	pHIPZ plasmid containing <i>PEX14</i> -2xHA- <i>PHO8</i> ^{N89} under the control of P_{ADH1} ; Zeo ^R , Amp ^R	This study

Table 3. Primers used in this study

Primers	Sequence (5' – 3')
RSAPex25-1	GGGGACAACTTTGTATAGAAAAGTTGCAAAGTCTGGATGG AGGCTTCATCTC
RSAPex25-2	GGGGACTGCTTTTTTTGTACAAACTTGAGCGTGGCATGCGG TTCATAGAAAC
RSAPex25-3	GGGGACAGCTTTCTTGTACAAAGTGGGAGTCTCTGCTCGC GTACAAGATC
RSAPex25-4	GGGGACAACTTTGTATAATAAAGTTGACTTGGAGCTGCTG TGCTTGTATG
attB1-Ptef1- forward	GGGGACAAGTTTGTACAAAAAAGCAGGCTGATCCCCACA CACCATAGCTTC
attB2-Ttef1-reverse	GGGGACCACTTTGTACAAGAAAGCTGGGTGCTCGTTTTTCG ACACTGGATGG
RSAPex25-5	CTGGATGGAGGCTTCATCTC
RSAPex25-6	GGAGCTGCTGTGCTTGTATG
Pex14FWD	GTCTCAACAGCCAGCAACGAC
R-GFP	CAGATGAACTTCAGGGTCAGC
ATG1_5'_fwd	GGGGACAACTTTGTATAGAAAAGTTGGGCTGGAGAACGCG GCAGATCC
ATG1_5'_rev	GGGGACTGCTTTTTTTGTACAAACTTGGGGAGGGGAAGGGT ACCTCTC
ATG1_3'_fwd	GGGGACAGCTTTCTTGTACAAAGTGGCCGCCACAAATGGT GAAGTCGATC
ATG1_3'_rev	GGGGACAACTTTGTATAATAAAGTTGCATCGAGCTTCTCG TTGCCCCGTGAC
pDEL_ATG1_fwd	ACAGGTCGTTGGTGACTTTAC
pDEL_ATG1_rev	CTTCTCGTTGCCCGTGACC
ATG1_cPCR_fwd	GGCTGGAGAACGCGGCAGAT
ATG1_cPCR_rev	GCGACCGTATCCACTGAACC
PRARM001	ATAGCGGCCGCTTGCAGGAAGTCGACGAAAT
PRARM002	CGGAAGCTTTTACTTGTACAGCTCGTCCA
RSA10fw	GAAGATCTATGGTGAGCAAGGGCGAGGAG
RSA11rev	GCGTGTCGACTTACTTGTACAGCTCGTCCATGCC
RSA12Fw	GGGGACAGCTTTCTTGTACAAAGTGGCCATGGTGAGCAAG GGCGAGGAG
RSA13Rev	GGGGACAACTTTGTATAATAAAGTTGCGATCTGAACCTCG ACTTTCTG
<i>att</i> P _{AOX} F	GGGGACAACTTTGTATAGAAAAGTTGGATCTCGACGCGGA GAACGATC
<i>att</i> P _{AOX} R	GGGGACTGCTTTTTTTGTACAAACTTGGTTTTTGTACTTTAG ATTGATGTCACC
BB-JK-037	GGGGACAAGTTTGTACAAAAAAGCAGGCTGTATGTCGTTT AACGACGATCTTTATAGGG

BB-JK-038	GGGGACCACTTTGTACAAGAAAGCTGGGTTATTCAGGCAG GGATTTAGCTCCTTTTCCG
AOX_StuI_fwd	CATAGAGGTCCTTGGCCATT
Pex25_SalI_rev	ACGCGTCGACTTAATTCAGGCAGGGATTTAGCT
AOX_up_fwd	TTCGAACCGAGCGAGTTGAA
Pex25_cPCR_rev	GCGTGGCATGCGGTTCATAG
BB-JK-037	GGGGACAAGTTTGTACAAAAAAGCAGGCTGTATGTCGTTT AACGACGATCTTTATAGGG
BB-JK-038	GGGGACCACTTTGTACAAGAAAGCTGGGTTATTCAGGCAG GGATTTAGCTCCTTTTCCG
AMO_sel_f	GTTGGCGAAAAGTCCAGAAG
mGFP_rev_check	AAGTCGTGCTGCTTCATGTG
Pex25_cPCR_fwd	CAAGCGACCTCGGCACAAGT
<i>Hind</i> III-Pex14	CCCAAGCTTATGTCTCAACAGCCAGCAAC
Pex14_HA-HA	TCCTGCATAGTCCGGGACGTCATAGGGATAGCCCGCATAG TCAGGAACATCGTATGGGTAGGCATTTCAGCTGCCACGCCG
HA-HA_Pho8	TACCCATACGATGTTCTGACTATGCGGGCTATCCCTATGA CGTCCCGGACTATGCAGGAATGCAACGGAACCAAGATCG
Pho8_PspXI (2)	CGCCTCGAGCCTAGCCTGTACCATCCGTGACCA
Pho8_PspXI_rev (2)	CGCCTCGAGCCTAGCCTGTA
Adh1_cPCR_fwd	TGTTGAGCAGGCTGATAACC
Pho8_cPCR_rev	CGCCGTCAAGCAGAGAATCG

Biochemical methods

Extracts of trichloroacetic acid treated cells were prepared for sodium dodecyl sulfate PAGE and Western blotting as detailed previously (Baerends et al., 2000; Laemmli, 1970). Blots were probed with rabbit polyclonal antisera against Pex3, Pex14 or pyruvate carboxylase (Pyc1). Secondary antibodies conjugated to horseradish peroxidase were used for detection. Pyc1 was used as a loading control. Blots were scanned by using a densitometer (Biorad GS-710) and quantified using ImageJ (version 1.37). Preparation of crude cell extracts was performed as described previously (van der Klei et al., 1991).

Fluorescence microscopy

Wide field images were captured at room temperature using a 100x1.30 NA objective (Carl Zeiss). Images were captured in media in which the cells were grown using a fluorescence microscope (Axio Scope A1; Carl Zeiss), Micro-Manager 1.4 software and a digital camera (Coolsnap HQ2; Photometrics). The GFP fluorescence was visualized with a 470/40 nm band pass excitation filter, a 495 nm dichromatic mirror, and a 525/50 nm band-pass emission filter. mCherry fluorescence was visualized with a 587/25 nm band pass excitation filter, a 605 nm dichromatic mirror, and a 647/70 nm band-pass emission filter. FM4/64 fluorescence was visualized with a 546/12 nm bandpass excitation filter, a 560 nm dichromatic mirror, and a 575-640 nm bandpass emission filter. The Vacuolar membranes were stained with FM4-64 by incubating cells at 37°C in 2 μ M FM4-64.

Image analysis was carried out using ImageJ and Adobe Photoshop CC 2015 software. To quantify peroxisomes, cells were grown in MM-M for 16 hours. Random images of cells were taken as a stack using a confocal microscope (LSM510, Carl Zeiss) and photomultiplier tubes (Hamamatsu Photonics) and Zen 2009 software (Carl Zeiss). Z-Stack images were made containing 12 (Fig 1.A) or 10 (Fig. 1B) optical slices and the GFP signal was visualized by excitation with a 488 nm argon ion laser (Lasos), and a 500-550 nm bandpass emission filter. Peroxisomes were quantified manually from two independent experiments (2 x 200 cells were counted).

Live cell imaging was performed on a Zeiss Observer Z1 using Axiovision software and a Photometrics Coolsnap HQ2 digital camera. Cells were grown on 1% agar containing MM-M/G and the temperature of the heating chamber XL was set at 37°C. Four z-axis planes were acquired for each time interval using 1 sec and 1.5 sec exposure times for GFP and mCherry, respectively.

Cryosectioning and immuno-gold labeling

For immune-EM, cells were fixed in 3% glutaraldehyde in 0.1 M cacodylate buffer, pH 7.2, for 1 h on ice and treated afterward with 0.4% sodium periodate (15 min) and 1% NH₄Cl (15 min). Upon embedding in 12% gelatin in phosphate buffer, pH 7.4, ~0.5 mm³ cubes were infiltrated overnight in 2.3 M sucrose in the same buffer. Cryosections of 60 nm were cut using a cryo diamond knife (Diatome) at -120°C in an ultramicrotome (Ultracut; Reichert). Sections were mounted on carbon-coated Formvar nickel grids. Pex14 and Pex3 were localized using polyclonal antibodies raised against Pex14 and affinity purified Pex3, and goat anti-rabbit antibodies conjugated to 10 nm gold (Aurion). Sections were stained with 2% uranyl oxalate, pH 7.0, for 10 min, briefly washed on three drops of distilled water, and embedded in 0.5% methylcellulose and 0.5% uranyl acetate on ice for 10 min before viewing them with a transmission EM microscope (CM12) (Slot and Geuze, 2007).

Acknowledgements

We are grateful to Arjen M. Krikken for his guidance and for construction of the *pex25* strain used in this project. This work was supported by grants from the Netherlands Organisation for Scientific Research/Chemical Sciences (NWO/CW) to AA (711.012.002) and the Marie Curie Initial Training Networks (ITN) program PerFuMe (Grant Agreement Number 316723) to IvdK.

References

- Agrawal, G., H.H. Shang, Z.-J. Xia, and S. Subramani. 2017. Functional regions of the peroxin Pex19 necessary for peroxisome biogenesis. *J. Biol. Chem.* 292:11547–11560. doi:10.1074/jbc.M116.774067.
- Baerends, R.J., K.N. Faber, A.M. Kram, J.A. Kiel, I.J. van der Klei, and M. Veenhuis. 2000. A stretch of positively charged amino acids at the N terminus of *Hansenula polymorpha* Pex3p is involved in incorporation of the protein into the peroxisomal membrane. *J. Biol. Chem.* 275:9986–9995.
- Baerends, R.J., F.A. Salomons, J.A. Kiel, I.J. van der Klei, and M. Veenhuis. 1997. Deviant Pex3p levels affect normal peroxisome formation in *Hansenula polymorpha*: a sharp increase of the protein level induces the proliferation of numerous, small protein-import competent peroxisomes. *Yeast Chichester Engl.* 13:1449–1463. doi:10.1002/(SICI)1097-0061(199712)13:15<1449::AID-YEA191>3.0.CO;2-Q.
- Cepińska, M.N., M. Veenhuis, I.J. van der Klei, and S. Nagotu. 2011. Peroxisome fission is associated with reorganization of specific membrane proteins. *Traffic Cph. Den.* 12:925–937. doi:10.1111/j.1600-0854.2011.01198.x.
- David, C., J. Koch, S. Oeljeklaus, A. Laernsack, S. Melchior, S. Wiese, A. Schummer, R. Erdmann, B. Warscheid, and C. Brocard. 2013. A Combined Approach of Quantitative Interaction Proteomics and Live-cell Imaging Reveals a Regulatory Role for Endoplasmic Reticulum (ER) Reticulon Homology Proteins in Peroxisome Biogenesis. *Mol. Cell. Proteomics.* 12:2408–2425. doi:10.1074/mcp.M112.017830.
- van Dijk, R., K.N. Faber, A.T. Hammond, B.S. Glick, M. Veenhuis, and J.A. Kiel. 2001. Tagging *Hansenula polymorpha* genes by random integration of linear DNA fragments (RALF). *Mol. Genet. Genomics MGG.* 266:646–656. doi:10.1007/s004380100584.
- Erdmann, R., and G. Blobel. 1995. Giant peroxisomes in oleic acid-induced *Saccharomyces cerevisiae* lacking the peroxisomal membrane protein Pmp27p. *J. Cell Biol.* 128:509–523. doi:10.1083/jcb.128.4.509.
- Faber, K.N., R. van Dijk, I. Keizer-Gunnink, A. Koek, I.J. van der Klei, and M. Veenhuis. 2002. Import of assembled PTS1 proteins into peroxisomes of the yeast *Hansenula polymorpha*: yes and no! *Biochim. Biophys. Acta.* 1591:157–162.
- Faber, K.N., P. Haima, W. Harder, M. Veenhuis, and G. Ab. 1994. Highly-efficient electrotransformation of the yeast *Hansenula polymorpha*. *Curr. Genet.* 25:305–310. doi:10.1007/BF00351482.
- Faber, K.N., A.M. Kram, M. Ehrmann, and M. Veenhuis. 2001. A Novel Method to Determine the Topology of Peroxisomal Membrane Proteins in Vivo Using the Tobacco Etch Virus Protease. *J. Biol. Chem.* 276:36501–36507. doi:10.1074/jbc.M105828200.
- Fagarasanu, M., A. Fagarasanu, Y.Y.C. Tam, J.D. Aitchison, and R.A. Rachubinski. 2005. Inp1p is a peroxisomal membrane protein required for peroxisome inheritance in *Saccharomyces cerevisiae*. *J. Cell Biol.* 169:765–775. doi:10.1083/jcb.200503083.

- Gleeson, M.A., and P.E. Sudbery. 1988. Genetic analysis in the methylotrophic yeast *Hansenula polymorpha*. *Yeast*. 4:293–303. doi:10.1002/yea.320040407.
- Huber, A., J. Koch, F. Kragler, C. Brocard, and A. Hartig. 2012. A Subtle Interplay Between Three Pex11 Proteins Shapes *De Novo* Formation and Fission of Peroxisomes. *Traffic*. 13:157–167. doi:10.1111/j.1600-0854.2011.01290.x.
- Kiel, J.A.K.W., M. Veenhuis, and I.J. van der Klei. 2006. *PEX* Genes in Fungal Genomes: Common, Rare or Redundant. *Traffic*. 7:1291–1303. doi:10.1111/j.1600-0854.2006.00479.x.
- van der Klei, I.J., W. Harder, and M. Veenhuis. 1991. Selective inactivation of alcohol oxidase in two peroxisome-deficient mutants of the yeast *Hansenula polymorpha*. *Yeast Chichester Engl*. 7:813–821. doi:10.1002/yea.320070806.
- Knoblach, B., X. Sun, N. Coquelle, A. Fagarasanu, R.L. Poirier, and R.A. Rachubinski. 2013. An ER-peroxisome tether exerts peroxisome population control in yeast. *Embo J*. 32:2439–2453. doi:10.1038/emboj.2013.170.
- Knoops, K., S. Manivannan, M.N. Cepińska, A.M. Krikken, A.M. Kram, M. Veenhuis, and I.J. van der Klei. 2014. Preperoxisomal vesicles can form in the absence of Pex3. *J. Cell Biol*. 204:659–668. doi:10.1083/jcb.201310148.
- Krikken, A.M., M. Veenhuis, and I.J. van der Klei. 2009. *Hansenula polymorpha pex11* cells are affected in peroxisome retention. *FEBS J*. 276:1429–1439. doi:10.1111/j.1742-4658.2009.06883.x.
- Laemmli, U.K. 1970. Cleavage of Structural Proteins during the Assembly of the Head of Bacteriophage T4. *Nature*. 227:680–685. doi:10.1038/227680a0.
- Leão-Helder, A.N., A.M. Krikken, I.J. van der Klei, J.A.K.W. Kiel, and M. Veenhuis. 2003. Transcriptional Down-regulation of Peroxisome Numbers Affects Selective Peroxisome Degradation in *Hansenula polymorpha*. *J. Biol. Chem*. 278:40749–40756. doi:10.1074/jbc.M304029200.
- Logan, M.R., L. Jones, and G. Eitzen. 2010. Cdc42p and Rho1p are sequentially activated and mechanistically linked to vacuole membrane fusion. *Biochem. Biophys. Res. Commun*. 394:64–69. doi:10.1016/j.bbrc.2010.02.102.
- Marelli, M., J.J. Smith, S. Jung, E. Yi, A.I. Nesvizhskii, R.H. Christmas, R.A. Saleem, Y.Y.C. Tam, A. Fagarasanu, D.R. Goodlett, R. Aebersold, R.A. Rachubinski, and J.D. Aitchison. 2004. Quantitative mass spectrometry reveals a role for the GTPase Rho1p in actin organization on the peroxisome membrane. *J. Cell Biol*. 167:1099–1112. doi:10.1083/jcb.200404119.
- Marshall, P.A., Y.I. Krimkevich, R.H. Lark, J.M. Dyer, M. Veenhuis, and J.M. Goodman. 1995. Pmp27 promotes peroxisomal proliferation. *J. Cell Biol*. 129:345–355. doi:10.1083/jcb.129.2.345.
- Mast, F.D., A. Jamakhandi, R.A. Saleem, D.J. Dilworth, R.S. Rogers, R.A. Rachubinski, and J.D. Aitchison. 2016. Peroxins Pex30 and Pex29 Dynamically Associate with Reticulons to Regulate Peroxisome Biogenesis from the Endoplasmic Reticulum. *J. Biol. Chem*. doi:10.1074/jbc.M116.728154.

- Motley, A.M., and E.H. Hettema. 2007. Yeast peroxisomes multiply by growth and division. *J. Cell Biol.* 178:399–410. doi:10.1083/jcb.200702167.
- Nagotu, S., A.M. Krikken, M. Otzen, J.A.K.W. Kiel, M. Veenhuis, and I.J. Van Der Klei. 2008a. Peroxisome Fission in *Hansenula polymorpha* Requires Mdv1 and Fis1, Two Proteins Also Involved in Mitochondrial Fission. *Traffic.* 9:1471–1484. doi:10.1111/j.1600-0854.2008.00772.x.
- Nagotu, S., R. Saraya, M. Otzen, M. Veenhuis, and I.J. van der Klei. 2008b. Peroxisome proliferation in *Hansenula polymorpha* requires Dnm1p which mediates fission but not de novo formation. *Biochim. Biophys. Acta BBA - Mol. Cell Res.* 1783:760–769. doi:10.1016/j.bbamcr.2007.10.018.
- Opaliński, Ł., J.A.K.W. Kiel, C. Williams, M. Veenhuis, and I.J. van der Klei. 2011. Membrane curvature during peroxisome fission requires Pex11. *EMBO J.* 30:5–16. doi:10.1038/emboj.2010.299.
- Rottensteiner, H., K. Stein, E. Sonnenhol, and R. Erdmann. 2003. Conserved Function of Pex11p and the Novel Pex25p and Pex27p in Peroxisome Biogenesis. *Mol. Biol. Cell.* 14:4316–4328. doi:10.1091/mbc.E03-03-0153.
- Saraya, R., A.M. Krikken, J.A.K.W. Kiel, R.J.S. Baerends, M. Veenhuis, and I.J. van der Klei. 2012. Novel genetic tools for *Hansenula polymorpha*. *FEMS Yeast Res.* 12:271–278. doi:10.1111/j.1567-1364.2011.00772.x.
- Shaner, N.C., R.E. Campbell, P.A. Steinbach, B.N.G. Giepmans, A.E. Palmer, and R.Y. Tsien. 2004. Improved monomeric red, orange and yellow fluorescent proteins derived from *Discosoma* sp. red fluorescent protein. *Nat. Biotechnol.* 22:1567–1572. doi:10.1038/nbt1037.
- Slot, J.W., and H.J. Geuze. 2007. Cryosectioning and immunolabeling. *Nat. Protoc.* 2:2480–2491. doi:10.1038/nprot.2007.365.
- Smith, J.J., and J.D. Aitchison. 2013. Peroxisomes take shape. *Nat. Rev. Mol. Cell Biol.* 14:803–817. doi:10.1038/nrm3700.
- Smith, J.J., M. Marelli, R.H. Christmas, F.J. Vizeacoumar, D.J. Dilworth, T. Ideker, T. Galitski, K. Dimitrov, R.A. Rachubinski, and J.D. Aitchison. 2002. Transcriptome profiling to identify genes involved in peroxisome assembly and function. *J. Cell Biol.* 158:259–271. doi:10.1083/jcb.200204059.
- Tam, Y.Y.C., J.C. Torres-Guzman, F.J. Vizeacoumar, J.J. Smith, M. Marelli, J.D. Aitchison, and R.A. Rachubinski. 2003. Pex11-related Proteins in Peroxisome Dynamics: A Role for the Novel Peroxin Pex27p in Controlling Peroxisome Size and Number in *Saccharomyces cerevisiae*. *Mol. Biol. Cell.* 14:4089–4102. doi:10.1091/mbc.E03-03-0150.